



# Properties of Gamma-Ray Burst Progenitor Stars

## Citation

Kumar, P., R. Narayan, and J. L. Johnson. 2008. "Properties of Gamma-Ray Burst Progenitor Stars." *Science* 321 (5887) (July 18): 376–379. doi:10.1126/science.1159003.

## Published Version

doi:10.1126/science.1159003

## Permanent link

<http://nrs.harvard.edu/urn-3:HUL.InstRepos:28487583>

## Terms of Use

This article was downloaded from Harvard University's DASH repository, and is made available under the terms and conditions applicable to Open Access Policy Articles, as set forth at <http://nrs.harvard.edu/urn-3:HUL.InstRepos:dash.current.terms-of-use#OAP>

## Share Your Story

The Harvard community has made this article openly available.  
Please share how this access benefits you. [Submit a story](#).

[Accessibility](#)

# Properties of Gamma-ray Burst Progenitor Stars

Pawan Kumar<sup>1</sup>, Ramesh Narayan<sup>2</sup> & Jarrett L. Johnson<sup>1</sup>

<sup>1</sup>Astronomy Department, University of Texas, Austin, TX 78712

<sup>2</sup>Harvard-Smithsonian Center for Astrophysics, Cambridge, MA 02138

**We determine some basic properties of stars that produce spectacular gamma-ray bursts at the end of their life. We assume that accretion of the outer portion of the stellar core by a central black hole fuels the prompt emission, and that fall-back and accretion of the stellar envelope later produces the plateau in the x-ray light curve seen in some bursts. Using x-ray data for three bursts we estimate the radius of the stellar core to be  $\sim (1 - 3) \times 10^{10}$  cm, and that of the stellar envelope to be  $\sim (1 - 2) \times 10^{11}$  cm. The density profile in the envelope is fairly shallow, with  $\rho \sim r^{-2}$ . The rotation speeds of the core and envelope are  $\sim 0.05$  and  $\sim 0.2$  of the local Keplerian speed, respectively.**

Observations of gamma-ray bursts (GRBs) suggest that the activity at the center of these explosions lasts for several hours (1,2). The most compelling evidence is provided by three bursts (3) – GRBs 060413, 060607A and 070110 – which show a sudden decline in their x-ray light curves (LCs) a few hours after the prompt burst (Fig. 1). The flux decline is by a factor of 10 or more and is much too sharp for the radiation to originate in an external forward shock (4); the most likely explanation is continued activity at the center of the explosion until at least the time of the decline. Additional evidence for continued activity of the central engine is provided by the x-ray flares seen in many GRBs (5-7), and also by those bursts whose x-ray & optical afterglow lightcurves (LCs) are mutually incompatible with a common origin (8, 9).

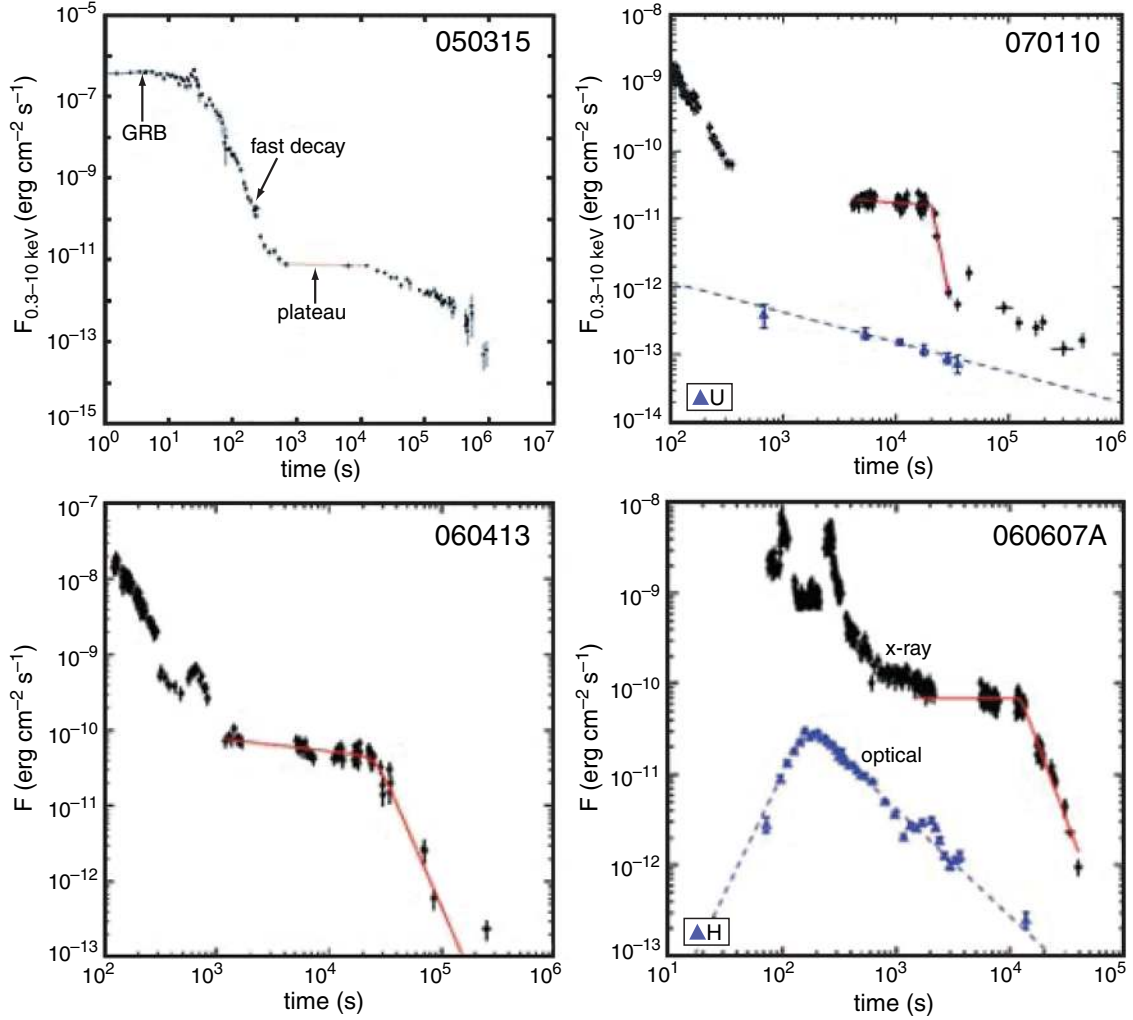


Figure 1: The top left panel (from Vaughan et al. 2006) shows the 0.3-10 keV band x-ray lightcurve (LC) of a typical long duration burst, GRB 050315. Four distinct phases are seen in the LC: the prompt GRB lasting for about a minute, an early steep decline lasting for  $\sim 10$  minutes, a plateau lasting until about  $10^4$  s, and a “normal” post-plateau decay. The top right panel (from Liang et al. 2007) shows x-ray and optical LCs for GRB 070110. The x-ray LC falls very sharply at the end of the plateau ( $t \sim 3 \times 10^3$  s), before switching to a normal decline, whereas the optical LC is a single power-law for the entire duration. The two lower panels (also from Liang et al. 2007) show the x-ray LCs of GRB 060413 and GRB 060607A. Note the complex x-ray LCs of these bursts, with flares, breaks, and plateaus. In contrast, the optical LCs of GRBs are typically smooth and simple, such as those of GRB 070110 and GRB 060607A, shown in the right panels in blue.

In fact, central engine activity is implicated whenever the observed flux variability time scale,  $\delta t$ , is much smaller than the time elapsed since the onset of explosion. The reason is that for a relativistic external shock causality dictates that  $\delta t \gtrsim R/2c\Gamma^2$ , and the time it takes for photons to arrive at the observer from a shock front at radius  $R$  that is moving with Lorentz factor  $\Gamma$  is also  $\sim R/2c\Gamma^2$ , i.e.  $\delta t/t \sim 1$  for external shocks.

In this paper, we adopt the collapsar model of GRBs (10,11), in which the inner part of the progenitor star collapses to a rapidly-spinning black hole (BH) and the remaining gas from the star accretes on to the BH and produces an ultra-relativistic jet. With a few plausible assumptions, we show that x-ray observations of the three bursts mentioned above (GRBs 060413, 060607A & 070110) may be inverted to infer the structure and rotation rate of their progenitor stars. These particular bursts were selected for this work because they have prominent x-ray plateaus which are almost certainly the result of central engine activity. Thus for these bursts, we have information on the power generation at the center covering an extended period of time, which enables us to determine the core and envelope structure of the progenitor star; only three bursts met this strict requirement of central engine activity dominated x-ray plateau. Some of the results we find regarding progenitor star properties – especially the core structure – apply to a much larger sample of bursts, as discussed at the end of the paper. We also note that optical emission was detected for two of the three bursts (Fig. 1). The optical LC is consistent with origin in the forward shock (FS). Moreover, for a reasonable set of parameters the amount of x-ray flux produced in the FS is found to be  $\sim 10^2$  times smaller than the flux observed during the plateau. Thus, there is consistency between a FS origin for the optical LC and central engine activity for the x-ray emission.

The panel on the left in Fig. 2 shows a schematic GRB x-ray lightcurve, which is based on the data shown in Fig. 1. The panel on the right outlines the basic features of our model and shows how the four phases of the LC are connected to corresponding zones in the progenitor

star.

We assume that the star has a core-envelope structure, as is common in stellar models. The bulk of the mass is in the stellar core.

Some of the mass in the core collapses directly to form a spinning BH and the rest accretes on the BH to produce the prompt GRB emission. Surrounding the inner zone is a second zone, which represents the transition region between the core and the envelope. This zone has a steeply falling density profile, and there is correspondingly a rapid decline in the x-ray flux. The outermost zone is a relatively low-density stellar envelope. Accretion of this gas produces the plateau in the LC. The drop in the x-ray flux at the end of the plateau, which can be sudden, corresponds to the time when the outermost layers of the envelope are accreted.

The fall-back time is the time it takes a parcel of gas in the progenitor star at radius  $r$  to fall to the center, and it is approximately equal to the free fall time (12),  $t_{\text{fb}} \sim 2(r^3/GM_r)^{1/2}$ , where  $M_r$  is the mass interior to  $r$ , and all times are in the frame of the GRB host galaxy. Let us assume that the accretion time  $t_{\text{acc}}$  of the gas in the disk is smaller than  $t_{\text{fb}}$  (see below). Then, at a given time  $t = 10^2 t_2$  s, the central engine will accrete gas that has fallen back from a radius  $r = 10^{10} r_{10}$  cm, where

$$r_{10} \sim 1.5 t_2^{2/3} M_{\text{BH},1}^{1/3}, \quad (1)$$

and  $M_{\text{BH},1}$  is the BH mass in units of  $10M_\odot$ . We are assuming here that the interior mass  $M_r$  is dominated by the BH. Let us suppose that the gas at radius  $r$  in the progenitor star has an angular velocity equal to a fraction  $f_\Omega$  of the local Keplerian velocity:

$$\Omega(r) = f_\Omega(r) \Omega_k(r) = f_\Omega(r) (GM_r/r^3)^{1/2}. \quad (2)$$

Then, the specific angular momentum  $j_* = 10^{18} j_{*,18} \text{ cm}^2 \text{ s}^{-1}$  of this gas is given by

$$j_{*,18}(r) \approx 3.8 M_{\text{BH},1}^{1/2} r_{10}^{1/2} f_\Omega(r) \approx 4.7 t_2^{1/3} M_{\text{BH},1}^{2/3} f_\Omega(r). \quad (3)$$

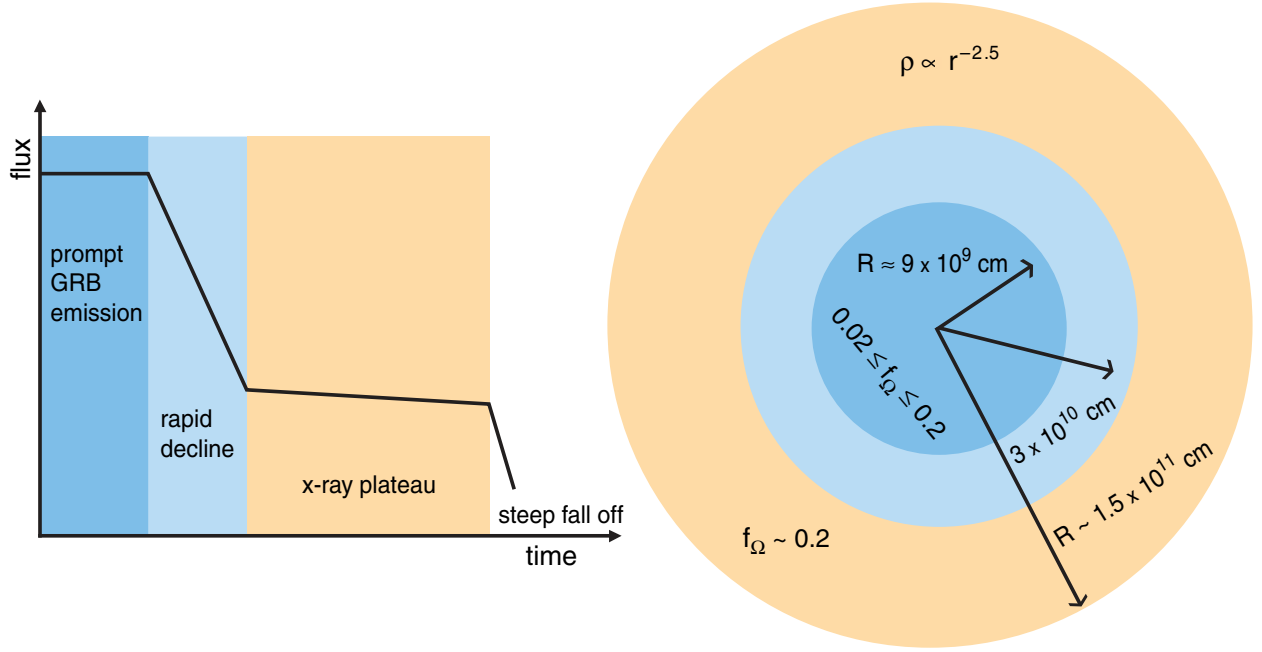


Figure 2: The panel on the left shows a schematic x-ray lightcurve with the following four segments: a prompt emission phase, a steep decline phase, a plateau phase, and a post-plateau phase. For the three GRBs considered in this work, the last phase has a steep and sudden decline. The panel on the right outlines our proposal for how the different segments in the LC are related to the accretion of corresponding zones in the progenitor star. The radii ( $r$ ) and spin parameters ( $f_{\Omega} \equiv \Omega/\Omega_k$ ) of the various zones are estimated from the x-ray data.

The gas will fall back toward the black hole until its angular momentum allows it to become centrifugally supported, at which point it becomes part of a thick accretion disk about the black hole. Its further in fall will then occur on the time scale at which viscous forces in the disk allow the orbit to decay.

The viscous accretion time of the fall-back gas after it has circularized is approximately equal to  $t_{\text{acc}} \sim 2/\alpha\Omega_k(r_d)$ , where  $\alpha = 0.1\alpha_{-1}$  is the viscosity parameter, and  $r_d \sim j_*^2/GM_{\text{BH}}$  is the radius at which gas with specific angular momentum  $j_*$  circularizes. Here we have assumed that the accretion disk is geometrically thick, which is generally true at the high mass accretion

rates expected in a collapsar (13). We thus have

$$t_{\text{acc}} \sim 10 \alpha_{-1}^{-1} f_{\Omega}^3(r) t_{\text{fb}} \sim 10 \alpha_{-1}^{-1} j_{d,18}^3 M_{\text{BH},1}^{-2} \text{ s}. \quad (4)$$

The first relation shows that the accretion time will be shorter than the fall-back time so long as  $f_{\Omega} \lesssim 0.4$  (for  $\alpha \sim 0.1$ ).

The jet power from the central engine is determined by the mass accretion rate  $\dot{M}_{\text{BH}}$  on to the BH, which is usually a small fraction of the mass fall-back rate  $\dot{M}_{\text{fb}}$  on to the accretion disk (the majority of the fall-back mass is expelled in a disk wind as it spirals in toward the BH [14]).

If the mass fall-back rate decreases suddenly at some time  $t_0$ , e.g., because of the transition from the stellar core to the envelope or when gas at the outer edge of the envelope has fallen back, then it can be shown by the conservation of mass and angular momentum that the accretion rate on the BH will decline with time as (15)

$$\dot{M}_{\text{BH}}(t) \sim \dot{M}_{\text{BH}}(t_0) [1 + 1.5(t - t_0)/t_{\text{acc}}]^{-2}, \quad t \geq t_0. \quad (5)$$

The exponent outside the square brackets is model-dependent and varies between  $-4/3$  and  $-8/3$ , depending on details; for definiteness, we choose  $-2$ . If  $t_{\text{acc}} \ll t_0$ , the effect of the above time dependence is that, in a log-log plot, the jet power will initially drop by a large factor  $\sim (t_0/t_{\text{acc}})^2$  within a time  $\sim t_0$ , and the power will then transition to an asymptotic decline  $\propto t^{-2}$ . This feature in the predicted LC plays an important role in our model. It is how we explain the sudden decline in the x-ray LC at the end of the prompt GRB and at the end of the plateau.

We apply these scaling relations to derive constraints on the stellar structure and rotation rate of GRB progenitors. A number of the features seen in GRBs can be explained naturally within the collapsar model as corresponding to the accretion of different portions of the progenitor star onto the central BH. Here we quantify the size, density, and rotation rate of the stellar core and envelope, as inferred from the observed timescales discussed above.

Observations with the x-ray telescope aboard the Swift satellite show that the flux in the 0.3–10 keV band of a typical long duration GRB is roughly constant for about 20 s (Fig. 1, top left panel), after which the x-ray LC undergoes a rapid decline as  $\sim t^{-3}$  or faster for about 5 minutes. Assuming that it takes  $\sim 30$  s for the BH to form, and adding to this the burst duration of 20 s, we estimate that the end of the main burst is approximately 50 s after the initiation of core collapse. By equation (1), the gas that falls back at this time comes from a radius  $\sim 9 \times 10^9 M_{\text{BH},1}^{1/3}$  cm. This radius must correspond to the outer edge of the innermost zone in the schematic stellar model shown in Fig. 2.

The subsequent steeply declining phase after the initial burst goes from  $t \sim 50 - 300$  s. In our model, this portion of the LC is associated with accretion of gas from the second zone in the star, the transition region between the core and the envelope where the density has a steep decline. Using the same argument as before, the outer radius of the second zone must be  $\sim 3 \times 10^{10} M_{\text{BH},1}^{1/3}$  cm.

A rapid decline in the x-ray LC requires a rapid decline in  $\dot{M}_{\text{BH}}$  (faster than  $\sim t^{-2}$ ), which is possible only when the disk is able to adjust quickly to a decrease in the mass-fall-back rate  $\dot{M}_{\text{fb}}$ . For an accretion flow to respond quickly to rapid changes in  $\dot{M}_{\text{fb}}$  at time  $t$  we must have  $t_{\text{acc}} \ll t$  (see Eq. 5). This condition provides an upper limit on the rotation speed in the core region of the progenitor star. The x-ray flux typically drops by a factor of  $\sim 10^3$  during the rapid decline phase at the end of the prompt burst (Fig. 1). Therefore, by Eq. 5, we require  $(250/t_{\text{acc}})^2 \gtrsim 10^3$  or  $t_{\text{acc}} \lesssim 8$  s at  $t \sim 50$  s. From Eq. 4, this means we must have  $f_{\Omega} \lesssim 0.2\alpha_{-1}^{1/3}$  at  $r \approx 10^{10}$  cm.

We can obtain a lower limit on  $f_{\Omega}$  in the stellar core by requiring that the angular momentum should be sufficiently large that the fall-back gas is able to form an accretion disk, i.e.,  $r_d \gtrsim 3R_g$ , where  $R_g \equiv GM_{\text{BH}}/c^2$  (note that the radius of the innermost stable circular orbit is  $2.3R_g$  for a BH with a spin parameter of 0.9). Since during core collapse a particle initially at  $r$  ends up



at a radius  $r_d \approx r[f_\Omega(r)]^2$ , where it is centrifugally supported, the condition  $r_d \gtrsim 3R_g$  yields  $f_\Omega(r) \gtrsim 0.02$ . An additional constraint on the core rotation rate is provided by the total energy of  $\sim 10^{52}$  erg observed in a typical GRB. Numerical simulations show that the efficiency for jet production from a rapidly rotating BH is about 1% (16), and therefore the total mass accreted by the BH should be about  $0.5M_\odot$ . This suggests that much of the mass within  $r \approx 10^{10}$  cm collapses directly to the BH, and therefore  $f_\Omega(r)$  is not much larger than 0.02; a reasonable estimate is  $f_\Omega \sim 0.05$  for  $r \lesssim 10^{10}$  cm.

A plateau in the x-ray LC is seen typically from  $\sim 3 \times 10^2 - 3 \times 10^3$  s (time in host galaxy rest frame). Gas falling on the central accretion disk during this time interval arrives from  $3 \times 10^{10} M_{\text{BH},1}^{1/3}$  cm  $\lesssim r \lesssim 1.5 \times 10^{11} M_{\text{BH},1}^{1/3}$  cm (Eq. 1). We suggest that the gas accreted during this phase comes from the envelope of the progenitor star, which means that the outer radius of the envelope must be  $\sim 1.5 \times 10^{11}$  cm. In principle, the plateau could be produced by supernova ejecta that failed to escape. However, such a model is unlikely to give the sharp cutoff which is seen in the x-ray LC at the end of the plateau in the three GRBs considered in this paper. For these GRBs at least, the plateau must arise from fall-back of the stellar envelope, which has a well-defined outer edge.

The density profile in the stellar envelope can be determined from the rate of decline of the x-ray flux during the plateau:  $f_x \propto t^{-\delta}$ ,  $\delta \sim 0.5$ . If the specific angular momentum of the gas in the envelope is constant, as might be the case if the envelope is convective, then the required density profile is  $\rho(r) \propto r^{-3(\delta+1)/2} \sim r^{-2.2}$  for  $\delta \sim 0.5$  (15). For a convective stellar envelope that is not very massive, we expect  $\rho \propto r^{-3/2}$  when gas pressure dominates and  $\rho \propto r^{-3}$  when radiation pressure dominates. The density profile we infer, assuming a constant specific angular momentum envelope, lies between these two limits. If the specific angular momentum increases with increasing radius, then a shallower decline of density is indicated; for instance,  $\rho \propto r^{-1.5}$  if the specific angular momentum increases with distance as  $\sim r^{3/4}$ . A solid-body rotation profile

for the envelope is ruled out because it requires an unphysical density structure in which  $\rho$  is almost independent of  $r$ .

The x-ray flux at the end of the plateau in GRBs 060413, 060607A & 070110 falls off sharply by a factor  $\sim 10^2$ . The fall-off occurs at  $t \sim 3 \times 10^3$  s and extends over a time  $\delta t \sim t$ . This steep fall-off requires the accretion time to be sufficiently short,  $t_{\text{acc}} \lesssim t/10 \sim 300$  s, which implies that  $j_{d,18} \lesssim 3\alpha_{-1}^{1/3} M_{\text{BH},1}^{2/3}$  and  $f_{\Omega}(r) \lesssim 0.2\alpha_{-1}^{1/3}$  at  $r \sim 1.5 \times 10^{11}$  (17, 18).

A lower limit for  $f_{\Omega}$  in the stellar envelope is obtained by the requirement that the in-falling gas should be able to form an accretion disk at the center; this implies  $f_{\Omega} \gtrsim 0.01$ . Another constraint comes from the fact that, apart from the flares discussed below, the x-ray LC during the plateau is usually quite smooth. This suggests that  $t_{\text{acc}}$  is fairly large (which plays the role of a smoothing time scale), and so  $f_{\Omega}$  is probably not much less than the upper limit of  $\sim 0.2$ .

After the sharp fall-off at the end of the plateau, the LC is expected to decline as  $\sim t^{-2}$  if the x-ray emission is dominated by jet luminosity associated with the debris disk (see Eq. 5). However, at these low flux levels the observed x-rays might be dominated by emission from shock-heated circumburst gas, i.e. external shock emission. In this case the flux will decline as  $\sim t^{-1}$ , e.g., GRB 070110 (Fig. 1).

For those GRBs where the x-ray LC makes a smooth transition at the end of the plateau phase,  $f_{\Omega}$  should be such that  $t_{\text{acc}} \sim t$ . For these systems, we require  $f_{\Omega} \sim 0.4$  near the outer edge of the progenitor star.

Rapid flares with short rise times are often seen during the plateau phase of the x-ray LC, and these provide additional constraints. A flare was seen at the beginning of the x-ray plateau in GRBs 060413 and 060607A, and at the end of the plateau in GRB 070110 (Fig. 1), with a rise time of order  $0.1t$ . Assuming the flares are produced by a disk instability, the rise time should be a factor of a few larger than the instability time scale  $t_{\text{inst}}$ . For a viscous instability  $t_{\text{inst}} \sim t_{\text{acc}}$  whereas for a dynamical (e.g., gravitational) instability  $t_{\text{inst}} \sim \Omega_k^{-1} \sim \alpha t_{\text{acc}}$ . Taking

the flare rise time to be  $\sim 5t_{\text{inst}} \sim 0.1t$  we find that  $f_{\Omega} \sim 0.1\alpha_{-1}^{1/3}$  in the stellar envelope if flares arise as a result of viscous instability, and  $f_{\Omega} \sim 0.3$  for a dynamical instability origin for flares. The amplitude of the flare  $f_{x,\text{flare}}/f_{x,\text{plateau}}$  can be at most  $\sim t_{\text{acc}}/t_{\text{inst}}$ . Thus, even in the limit of a dynamical instability, the amplitude is limited to  $\sim \alpha^{-1} \sim 10$ . Much larger flare amplitudes (e.g., in GRB 060526 [5]) might suggest an unusually small value of the viscosity parameter  $\alpha$ . Alternatively, these flares may be caused by a sudden increase in the mass fall-back rate, though such an event is not easy to visualize in our model.

The decay time of flares is expected to be of order  $t_{\text{acc}}$ , as this is the time scale on which a transient enhancement of the accretion rate, regardless of its origin, will subside. A noticeable difference between the x-ray plateau and the prompt emission is that LCs are typically more variable during the burst, and this raises a question as to why the central engine behaves differently during the two phases. Part of the difference is that instability timescales are longer when the outer envelope of the star, with a larger specific angular momentum, is accreted. Another factor is that, during the plateau phase, the jet propagates through an already evacuated cavity and is less prone to fluctuating baryon loading.

An upper limit on the stellar radius  $R_*$  is provided by the requirement that the energy expended as the relativistic jet makes its way out of the star not exceed the energy initially injected into the jet. Using results in (19, 20) we find  $R_* \lesssim 5 \times 10^{11}$  cm. Our radius estimates are consistent with this limit.

A possible way to get a handle on the mass of the GRB progenitor star is via the total energy produced in the explosion. The mass accreted during the prompt burst was estimated in §2.2.2 to be  $\sim 0.5M_{\odot}$ . The energy release during the plateau is typically about 10% of that in the prompt burst, i.e.,  $\sim 10^{51}$  erg (assuming the same beaming factor and efficiency as during the initial burst). Therefore, the mass accreted by the BH is only  $\sim 0.03M_{\odot}$ . Even after allowing for the fact that only a small fraction  $\sim (r_d/R_g)^{1/2} \sim 10^{-2}$  of the total fall-back mass actually reaches

the BH, the rest being carried away in a disk wind, we estimate that the mass of fall-back gas in the plateau phase is no more than a few  $M_{\odot}$ . The mass of the BH can be constrained because much of the mass within  $\sim 10^{10}$  cm collapses to the BH; for an evolved star this mass is about  $5M_{\odot}$ . Thus we estimate the mass of the GRB progenitor star to be  $M_* \sim 10M_{\odot}$ , plus whatever mass is ejected in the accompanying supernova explosion, which we are unable to constrain.

Figure 2 summarizes our primary results on the properties of GRB progenitor stars. The three bursts we considered in this paper are notable in that they have a steep fall-off of x-ray flux at the end of the plateau phase. These bursts provide the most detailed information on the properties of their progenitor stars. Many of our arguments and results, especially those in which we use the prompt burst and subsequent steep fall-off to infer the properties of the stellar core, should apply to any long duration GRB. Similarly, our discussion of the x-ray plateau can be applied to other bursts that have plateaus in their x-ray LCs which are produced by continuous accretion activity i.e., those GRBs that show a simple power-law decline of the optical LC and a plateau in the x-ray; these comprise roughly one third of the long GRBs observed by Swift.

## 1 References and Notes

1. The possibility of a long lived central engine activity was suggested<sup>2</sup> soon after the discovery of GRB afterglow emission.
2. J.I. Katz, T. Piran, R. Sari, *Phy. Rev. Letters*, 80, 1580 (1998)
3. E-W Liang, B-B Zhang, B. Zhang arXiv:0705.1373 (2007)
4. E. Nakar, J. Granot, astro-ph/0606011 (2006)
5. D. Burrows et al., *Science*, 309, 1833 (2005)
6. G. Chincarini, astro-ph/0702371 (2007)

7. B. Zhang, ChJAA 7, 1 (2007)
8. Y. Fan, T. Piran, MNRAS 369, 197 (2006)
9. A. Panaitescu et al. MNRAS 369, 2059 (2006)
10. S.E. Woosley, ApJ 405, 273 (1993)
11. B. Paczynski, ApJ 494, L45 (1998)
12. The factor of 2 in the expression for  $t_{\text{fb}}$  accounts for the time it takes signals to travel to  $r$  and to communicate the loss of pressure support at the center.
13. R. Narayan, T. Piran and P. Kumar, ApJ 557, 949 (2001)
14. K. Kohri, R. Narayan and T. Piran, ApJ 629, 341 (2005)
15. P. Kumar, R. Narayan and J. L. Johnson, to appear in MNRAS (2008)
16. J.C. McKinney, ApJ 630, L5 (2005)
17. Note that the decline of the LC cannot be steeper than  $\sim t^{-3}$ ; this is due to late arriving photons from outside the relativistic beaming angle of  $\Gamma^{-1}$  (18). Therefore, we can only place an upper limit on  $f_{\Omega}$  from the steepness of the decline after the x-ray plateau.
18. P. Kumar and A. Panaitescu, ApJ 541, L51 (2000)
19. E. Ramirez-Ruiz, A. Celotti, M.J. Rees, MNRAS 337, 1349 (2002)
20. C.D. Matzner, MNRAS 345, 575 (2003)